Desalination and Water Treatment
www.deswater.com

doi: 10.5004/dwt.2022.29067

279 (2022) 48–54
December

Removal of cadmium from aqueous solution by hybrid reinforced porous gelled beads based on SA/PVA/Al-Mt and $CaCO_3$

Ahlem Hattali[a,b,*], Omar Bouras[b], Salah Hanini[a]

[a]*Laboratory of Biomaterials and Transport Phenomena, Yahia Fares University, Medea 26000, Algeria, email: ahl_hattali@yahoo.fr (A. Hattali)*
[b]*Water Environment and Sustainable Development Laboratory, Blida1 University, BP270-09000, Algeria*

Received 11 June 2022; Accepted 19 September 2022

ABSTRACT

Two classes of hybrid reinforced porous gelled beads were fabricated based on sodium alginate (SA), polyvinyl alcohol (PVA), aluminum-pillared montmorillonite (Al-Mt) and calcium carbonate ($CaCO_3$). F1 (SA, PVA and $CaCO_3$) and F2 (SA, PVA, Al-Mt and $CaCO_3$) were generated and used for the removal of Cd^{2+} ions from aqueous solutions. A secondary aim was to enhance the mechanical stability of the alginate gels beads and increase the specific surface area of the adsorbate. The beads were characterized by Fourier-transform infrared spectroscopy and by physico-chemical measurements. Results showed that the application of F1 and F2 beads by discontinuous adsorption had high adsorption efficiency with Cd^{2+} elimination rates of the order of 77% and 96% in 1 h, respectively. The study indicated that the effect of pH in the range (3 to 9) seemed negligible with the F1 matrix unlike the F2 matrix, which showed an increase of Cd^{2+} removal of 74% to 96%. The kinetic studies as well as those of the Cd^{2+} adsorption isotherms on these new hybrid reinforced porous beads F1 and F2 agreed well with the pseudo-second-order model and Freundlich model, respectively.

Keywords: Aluminum-pillared montmorillonite; Gelled porous beads; Adsorption; Cadmium

1. Introduction

The development of techniques dedicated to the removal of toxic substances such as heavy metal ions from wastewater has proven to be a difficult task [1]. Cadmium (Cd) is one of heavy metals which can be found in wastewater streams from electroplating, smelting, paint pigments, batteries, fertilizers, mining and alloy industries [2,3]. For a human, exposure of Cd at high concentration can damage major organs (kidneys, liver, lungs), immune and reproductive systems, and among others [4,5]. With these, removal of Cd from any water body is important and pressing.

Polyvinyl alcohol (PVA) has been successfully used as an adsorbent towards heavy metal ions, anionic and cationic dyes due to the abundance of free hydroxy (–OH) and acetate (–O–CO–CH_3) groups residing on the PVA polymeric chains [6]. Due to the many properties in terms of durability, biocompatibility, tensile strength and degradability that PVA can offer, it has been incorporated into several types of materials such as alginates, zeolites, polyaniline, clays, oxide of graphene [6].

Calcium carbonate ($CaCO_3$) in limestone is known for efficiently removing heavy metals in aqueous solution up to 99% [7,8]. An alternative source of $CaCO_3$ is the eggshells. The chicken eggshells as an adsorbent could remove Cd in an aqueous solution up to 73%. The optimum adsorption capacity was 146 $mg{\cdot}g^{-1}$ obtained at 150 $mg{\cdot}L^{-1}$ initial concentration, 75 min contact time, 0.75 g adsorbent dose, and pH 6 at room temperature [9]. In recent years, a new family of porous beads based on $CaCO_3$ has proven its great adsorption properties towards certain heavy metals from aqueous solutions [10].

* Corresponding author.

Presented at the First International Congress of Energy and Industrial Process Engineering (ICEIPE'22) 23–25 May 2022, Algiers, Algeria

1944-3994/1944-3986 © 2022 Desalination Publications. All rights reserved.

The adsorption of cadmium ions from aqueous solution on to alginate–calcium carbonate composite material was investigated previously in batch mode. The obtained results showed that sorption of Cd^{2+} ions is a viable process with very encouraging recovery of the pollutant [11].

The maximum adsorption capacity of native chitosan flakes for the removal of cadmium in aqueous solution is 10 $mg \cdot g^{-1}$, similar to that of commercial activated carbon (10.3 $mg \cdot g^{-1}$). On the other hand for the chitosan/activated carbon nanocomposite, it is much higher since it reaches a value of 52.63 $mg \cdot g^{-1}$ [12].

The adsorption capacity of cadmium can be improved by supporting chitosan on solid supports such as bentonite [13] and magnetic nanoparticles [14]. In this context, a new chitin hydrogel of calcium nano-carbonate ($CaCO_3$) doped in situ as a sorbent was synthesized and used to remove Cu(II) and Cd(II) ions. The removal efficiencies of these two metal ions Cu(II) and Cd(II) after five successive adsorption cycles gave yields greater than 90%, thereby indicating the high stability and reproducibility of this composite material [15].

This present study concerns the preparation of a new generation of reinforced and porous hybrid gelled beads characterized by exceptional properties in terms of rigidity, porosity, specific surface area and above all strong sorption properties towards Cd^{2+} cations from solutions aqueous.

The strategy adopted in this study involves the use of stoichiometric mixtures of compatible materials such as natural polymers (sodium alginate), synthetic polymers (PVA), $CaCO_3$ and Al-pillared montmorillonite (Al-Mt) was produced under previously optimized conditions [16].

2. Materials and methods

All chemicals used were analytical reagent grade.

2.1. Preparation of aluminum-pillared montmorillonite (Al-Mt)

The bentonite employed, which was supplied by ENOF (National Company for Useful Substances and Non-Ferrous Products), was characterized previously [17]. The Al-Mt type matrices were characterized by basal spacing of around 1.8 nm, specific surface areas between (250 and 300) $m^2 \cdot g^{-1}$ and good thermal stability at 500°C [16]. The entire pillared clay preparation protocol is summarized in Fig. 1.

2.2. Preparation of hybrid reinforced porous gelled beads

Two classes of hybrids gelled beads (F1 and F2) were prepared by dispersing the mixture of powders of the selected products (sodium alginate, calcium carbonate and/or aluminum-pillared montmorillonite) in distilled water. Continuous stirring for 1 h ensured the homogenization of each mixture. To obtain stronger beads, PVA solutions were added to the two original dispersions and stirred continuously for 1 h. As shown in Fig. 2, the mixture was poured into a solution of boric acid and calcium chloride by drip system in order to produce the reinforced and porous hybrid gelled beads. These beads were submerged in hydrochloric acid solution. The resultant beads were rinsed and stored in distilled water.

2.3. Characterization of hybrid reinforced porous gelled beads

The sizes of the resulting beads were measured using a digital caliper. The zero charge points (pH_{ZPC}) of all the sorbents were determined by potentiometric dosage according to the protocol of Kummert and Stumm [18]. The apparent densities of these hybrid gelled beads were determined according to the gravimetric method. The water contents of beads were calculated according to Eq. (1):

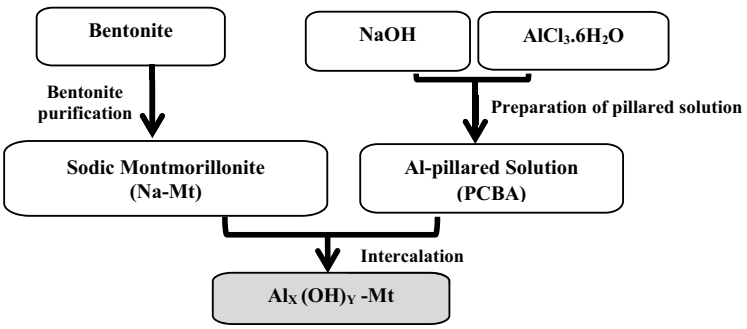

Fig. 1. Flowchart showing the different experimental methods of processing and modifying the used bentonite.

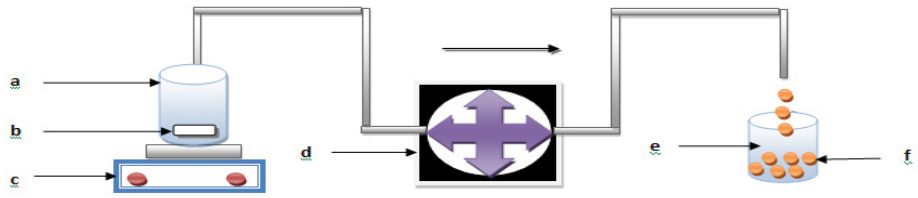

Fig. 2. Diagram of the experimental device illustrating the preparation of the hybrid reinforced porous gelled beads: (a) mixture of (AS/PVA/$CaCO_3$/Al-Mt), (b) magnetic bar, (c) magnetic stirrer, (d) peristaltic pump, (e) solution of $CaCl_2$ and boric acid and (f) gelled beads.

$$\text{Water content} = \left(\frac{\left(W_s - W_d\right)}{W_d} \right) \times 100 \quad (1)$$

where W_s is the weight of the water-swollen beads and W_d the weight of the dried beads.

The Fourier-transform infrared spectroscopy (FTIR) recorded in the range of 400–4,000 cm^{-1} (Instrument 8900-SHIMADZU) were carried out on the powders (pure alginate, Al-Mt, PVA, $CaCO_3$) and dried hybrid reinforced porous beads (sample F2). The effect of pH effect was studied in the range of 3–9 for 24 h using an initial concentration of Cd^{2+} solution equal to 10 $mg{\cdot}L^{-1}$. The chemical stability test is performed according on the following process: a mass of 1 g of hybrid reinforced porous gelled beads was immersed in a bottle containing 50 mL of hydrochloric acid or sodium hydroxide solutions. The pH range of the solution is varied from 3 to 13. The gel beads were allowed to stand without shaking for 7 d at T = 20°C ± 2°C.

2.4. Batch adsorption experiment

2.4.1. Kinetic studies

A mass of 0.5 g of wet sorbent beads was mixed with 50 mL of cadmium solution (10 $mg{\cdot}L^{-1}$) in a medium at pH 5.8. The suspensions were stirred at 225 rpm at ambient temperature. The adsorption kinetics study was conducted by taking samples at various time intervals ranging from 0 to 7 h. Atomic absorption spectrometry (type: iCE3500 AA System) was used to determine Cd^{2+} concentration at wavelength 228.8 nm. The adsorption capacities of Cd^{2+} on the beads were calculated according to Eq. (2):

$$q_t = \left(C_0 - C_t\right) \times \frac{V}{W_d} \quad (2)$$

where q_t is the adsorbed quantity of Cd^{2+} at time t ($mg{\cdot}g^{-1}$), C_0 and C_t: the initial and final concentrations ($mg{\cdot}L^{-1}$), V: the solution volume (L), and W_d: the weight of the dried beads (g).

2.4.2. Adsorption isotherms

Samples of wet hybrid reinforced porous gelled beads varying from 0.5 to 2.5 mg were mixed with 50 mL of the Cd^{2+} solution (C_0 = 10 $mg{\cdot}L^{-1}$, pH = 5.8), and stirring at 225 rpm for 140 min.

Adsorbed quantities at equilibrium q_e are calculated from the following equation:

$$q_e = \left(C_0 - C_e\right) \times \frac{V}{W_d} \quad (3)$$

where q_e: adsorbed quantity of Cd^{2+} at equilibrium ($mg{\cdot}g^{-1}$); C_0 and C_e: initial and equilibrium concentrations of Cd^{2+} ($mg{\cdot}L^{-1}$); V: solution volume (L); W_d: weight of the dried beads (g).

The nonlinear forms of the classical models (Freundlich and Langmuir) were used for modeling the adsorption isotherms, which are represented respectively by the following equations:

$$q_e = K_F C_e^n \quad (4)$$

$$q_e = \frac{q_m K_L C_e}{\left(1 + K_L C_e\right)} \quad (5)$$

where q_e and q_m: are respectively, equilibrium and maximum adsorption capacities ($mg{\cdot}g^{-1}$); C_e: equilibrium.

concentration of Cd^{2+} ($mg{\cdot}L^{-1}$); K_F: parameter relating to the adsorption capacity; n: parameter relating to the distribution of adsorption energies; K_L: ratio between adsorption and desorption rate constants.

All calculations have been established by software Origine.8.

3. Results and discussion

3.1. Characterization of hybrid reinforced porous gelled beads

The results related to the particle size distribution, the density, the water content and the pH_{ZPC} for the hybrid reinforced porous gelled beads are given in Table 1. Fig. 3 show the corresponding photographies of the obtained hybrid reinforced porous gelled beads (F1 and F2).

The results of the chemical stability tests clearly show that the beads are stable in acidic and neutral solutions but collapse after one week in a basic solution. The corresponding Fig. 4 shows that the effect of pH in the range 3–9 is negligible on elimination rate of Cd^{2+} by SA-PVA-$CaCO_3$ (F2) beads. Nevertheless, the removal rate is improved from 74% to 96% in the same pH range (3 to 9) by SA-PVA-$CaCO_3$-Al-Mt (F2) beads. The FTIR spectral analysis (Fig. 5) was performed on the powders (pure alginate, Al-Mt, PVA, $CaCO_3$) as well as on the dried hybrid reinforced porous beads (sample F2). Results show a strong absorption band around 3,420 cm^{-1}, corresponding to O–H stretching vibrations [19–21]. The two bands at 1,038 and 520 cm^{-1} have been attributed to the stretching and bending vibrations of the SiO, SiO–Al in the montmorillonite structure, respectively [22]. In the alginate spectrum, two specific strong absorption bands appear at 1,636 and 1,407 cm^{-1}; these are attributed to asymmetric and symmetric stretching vibrations of the COO^- groups, respectively [23,24]. The C–H stretching in PVA

Table 1
Physical characterization of hybrid reinforced porous gelled beads

Samples (Code)	Beads diameter (mm)	Water content (%)	Density	pH_{ZPC}
SA-PVA-$CaCO_3$ (F1)	3.48	95.46	1.30	7.00
SA-PVA-$CaCO_3$-Al-Mt (F2)	2.94	87.20	1.42	7.00

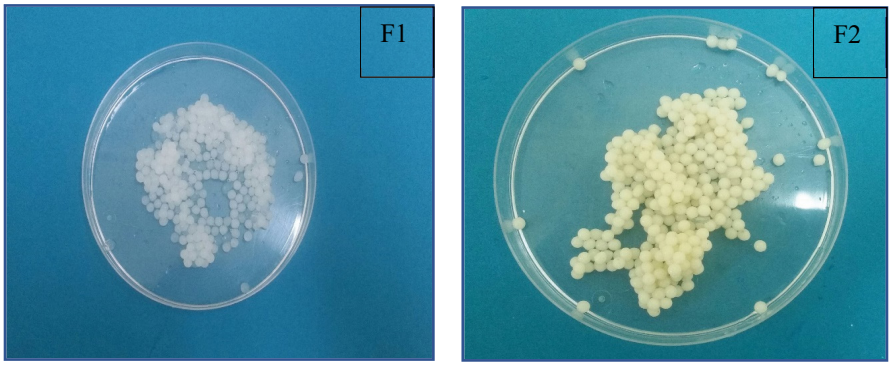

Fig. 3. Photographies of the hybrid reinforced porous gelled beads (F1 and F2).

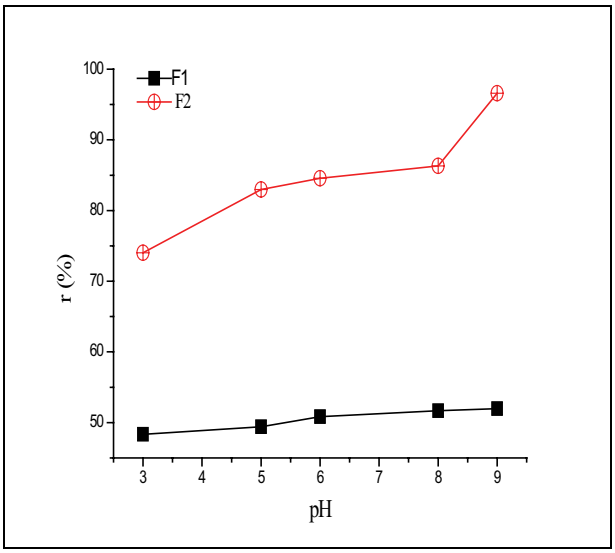

Fig. 4. pH effect on Cd^{2+} adsorption by hybrid reinforced and porous gelled beads.

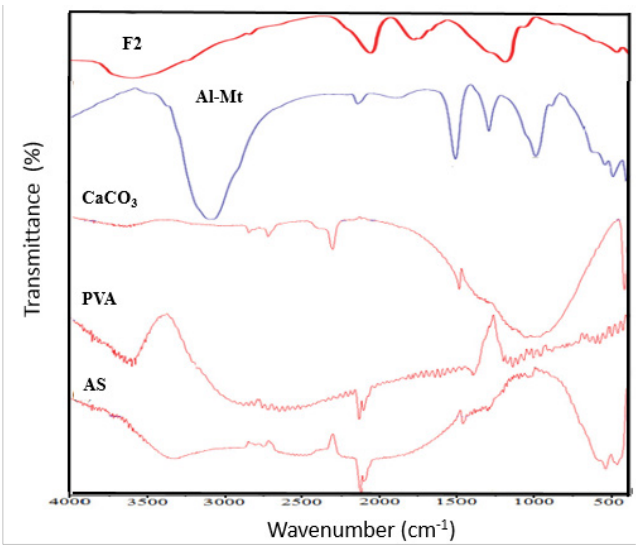

Fig. 5. FTIR spectrum of different sorbent.

indicates an absorption band at 1,440 cm^{-1} [19–21]. The anion carbonate in $CaCO_3$ indicates an absorption band at 1,400 cm^{-1} [21]. The comparative study of the superposed FTIR spectra clearly indicated the immobilization of both Al-Mt particles, $CaCO_3$ and PVA fractions in the alginate beads, thereby confirming the heterogeneous character of these new hybrid reinforced and porous gelled beads.

3.2. Modeling of sorption kinetics

Fig. 6 presents the sorption kinetics of Cd^{2+} on the hybrid reinforced porous gelled beads. The corresponding results indicate strong adsorption from the first few minutes where the adsorption capacity increases slightly with increasing contact time to reach an equilibrium contact time of around 60 min for the two formulations used (SA-PVA-$CaCO_3$ beads (F1) and SA-PVA-$CaCO_3$-Al-Mt beads (F2)).

The corresponding experimental results were modeled by applying pseudo-first-order and pseudo-second-order kinetic models. As shown in Table 2 and Fig. 7, the kinetic behavior of Cd^{2+} adsorption on hybrid reinforced porous gelled beads was well characterized by the pseudo-second-order model. The calculated values of adsorbed quantity at equilibrium from the pseudo-second-order graph were close to those determined experimentally. The correlation coefficients (R^2) were considered satisfactory, which

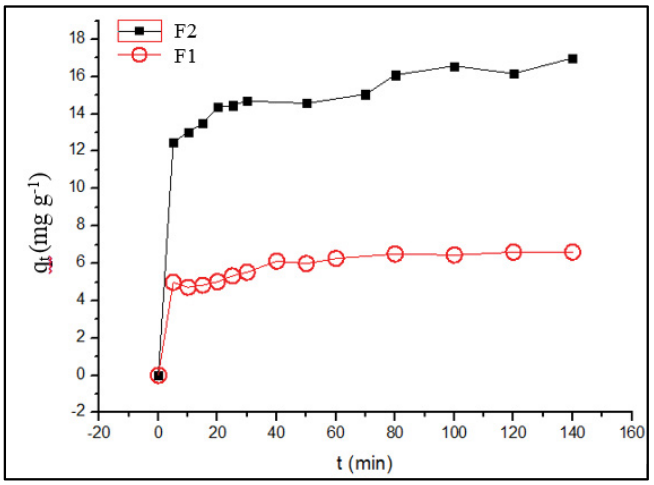

Fig. 6. Sorption kinetics curves of Cd^{2+} on the two prepared beads.

Table 2
Parameter values related to Cd^{2+} adsorption kinetics on the prepared beads

Parameters	$q_{e,exp}$ (mg·g^{-1})	Pseudo-first-order model			Pseudo-second-order model		
		$q_{e,cal}$ (mg·g^{-1})	K_1 (min^{-1})	R^2	$q_{e,cal}$ (mg·g^{-1})	K_2 (g·g^{-1}·min^{-1})	R^2
SA-PVA-$CaCO_3$ (F1)	6.60	9.32	–0.057	0.857	6.86	0.028	0.998
SA-PVA-$CaCO_3$-Al-Mt (F2)	17.00	2.88	–0.01	0.819	16.70	0.013	0.996

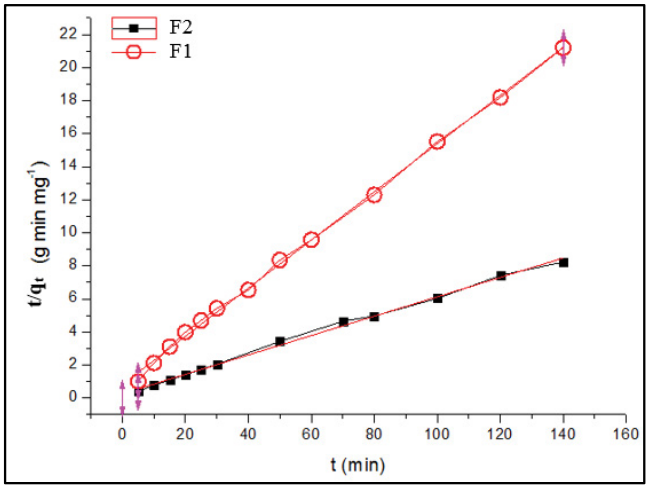

Fig. 7. Modeling of Cd^{2+} kinetic sorption by pseudo-second-order.

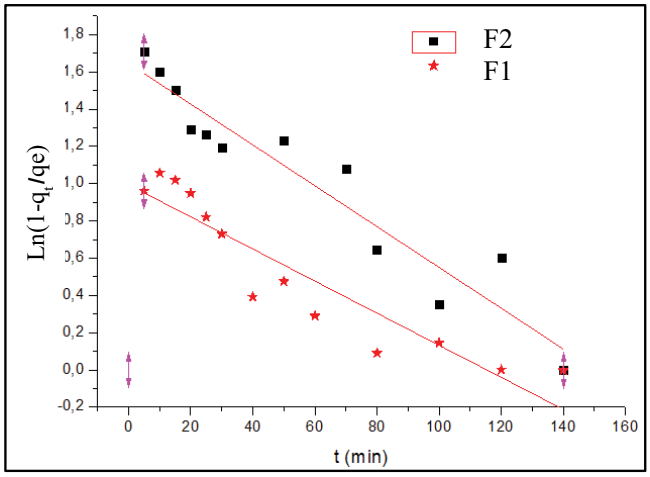

Fig. 8. Modeling plots of intraparticle diffusion of Cd^{2+} on beads, using Crank model [30].

Table 3
Kinetic parameters of several adsorbents

Sample	Pseudo-second-order			Equilibrium time (h)	Conditions	References
	$q_{e,cal}$ (mg·g^{-1})	K_2 (g·g^{-1}·min^{-1})	R^2			
SA-PVA-$CaCO_3$	6.86	0.028	0.998	1	pH 5.8, 0–140 min, 25°C, 10 mg/L	This study
SA-PVA-$CaCO_3$-Al-Mt	16.70	0.013	0.996	1	pH 5.8, 0–140 min, 25°C, 10 mg/L	This study
Levextrel resin	22.3	6.6×10^{-1}	0.999	1.5	pH 6.5, 0.083–5 h, 25°C, 100 mg/L	[26]
Eggshells	8.3	1.08	0.994	1.0	pH 5.5, 0.083–1.0 h, 25°C, 100 mg/L	[27]
Bca	64.9	1.6×10^{-1}	1.000	1.0	pH5.0, 0.17–23.3 h, 25°C, 166 mg/L	[28]
MC151.8	408.1	1.4×10^{-1}	0.968	2.0	pH 6.0–6.5, 0.017–6.0 h, 20°C, 500 mg/L	[29]

means that the rate of the adsorption of Cd^{2+} depends on the concentration factor [25].

Table 3 draws up a comparison between the adsorption capacity values ($q_{e,cal}$) of some adsorbents of different natures reported in the literature and those obtained by the hybrid reinforced gelled beads in this present study. These results clearly show that the $q_{e,cal}$ values vary depending on the nature of the sorbent. This comparison also shows that the F2 matrix (SA-PVA-$CaCO_3$-Al-Mt) has a sorption affinity towards Cd^{2+} ions in aqueous solutions.

The kinetic data was also analyzed using Crank [30] model to determine the pore diffusion coefficient, using respectively Eq. (6):

$$\frac{q_t}{q_e} = 1 - \left(\frac{6}{\pi^2}\right)\exp\left(\frac{-D_p\pi^2}{a^2 t}\right) \quad (6)$$

where q_e (mg·g^{-1}) and q_t (mg·g^{-1}) represent the adsorbed quantity of Cd^{2+} at equilibrium; and at time t, respectively; and a is the bead diameter.

Fig. 8 as well as Table 4 show the results of D_p and R^2 for Cd^{2+} adsorption on the both beads (F1 and F2). We can see that de pore diffusion coefficient of F1 is almost a same as F2.

3.3. Modeling of adsorption isotherms

Fig. 9 shows the cadmium adsorption isotherms on the hybrid reinforced porous gelled beads. The appearance of these isotherms is of the S1 type in which the direction of the adsorbate on the surface is vertical, due to the solute-solute attraction forces as indicated by the classification established by Giles et al. [31].

The modeling of adsorption isotherms is essential to characterize the adsorbate–adsorbent interactions. The

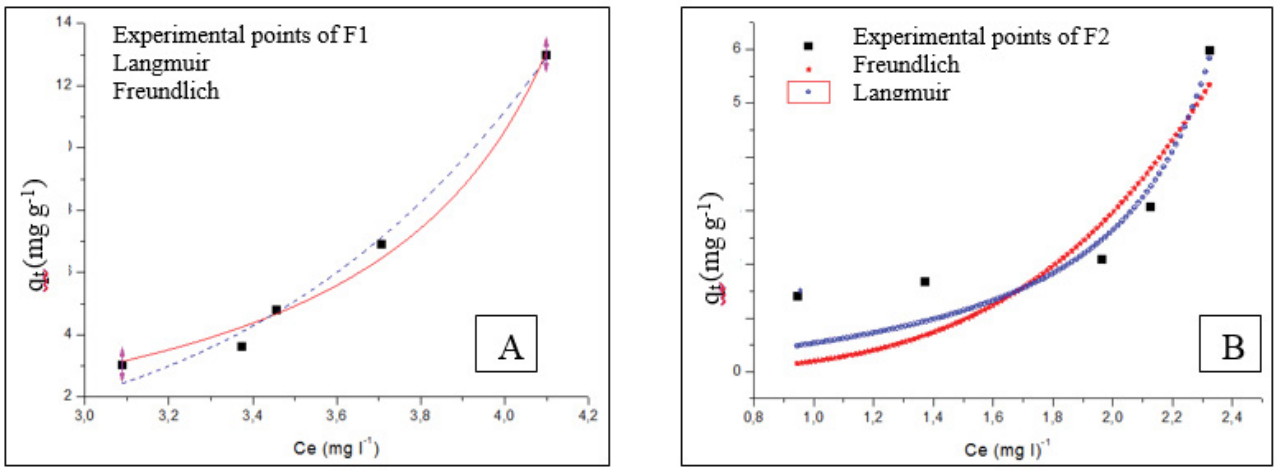

Fig. 9. Modeling of Cd^{2+} adsorption isotherm: (A) sample F1 and (B) sample F2.

Table 4
Modeling of intraparticle diffusion of Cd^{2+} on the beads

Mathematical model	Crank model	
Parameters	$D_p \cdot 10^8$ ($m^2 \cdot s^{-1}$)	R^2
AS-PVA-$CaCO_3$	1.056	0.855
AS-PVA-Al-Mt-$CaCO_3$	0.955	0.905

Table 5
Modeling parameters of Cd^{2+} adsorption isotherms on the beads

Mathematics models	Parameters	F1	F2
Freundlich	K_F	0.003	0.196
	n	5.896	3.921
	R^2	0.987	0.623
Langmuir	q_m (mg·g^{-1})	12.99	5.99
	K_L	–0.218	–0.370
	R^2	0.987	0.838

Langmuir model indicates that chemisorption by a monolayer coating is dominant [32,33], but the Freundlich model is developed rather for non-uniform surface adsorption [34].

In this study, the classical models of Freundlich (nonlinear) and Langmuir (nonlinear) were employed. At this stage and in order to take into account all the experimental points, it is well recommended to use the non-linearization in the mathematical modeling of the results than the linearization.

According to Table 5 and Fig. 9, the obtained coefficient of correlation R^2 from Langmuir model is higher than Freundlich model, but the obtained K_L values are negatives. Under such conditions, only the Freundlich model seems to give more satisfactory results related to the two types of prepared hybrid reinforced porous gelled beads (F1 and F2) in comparison with the other Langmuir model. This heterogeneous sorption process that took place on the surface of the adsorbent as there is no uniformity in the distribution of binding sites and therefore suggests a degree of nonlinearity between the concentration of the solution and the concentration of Cd ions in the surface of the adsorbent [33].

4. Conclusion

The removal rate of Cd^{2+} in aqueous solution by the hybrid reinforced porous gelled beads was improved by about 20% after the introduction of the Al-Mt fraction, which showed good chemical stability in acidic medium. A good correlation coefficient was obtained for the pseudo-second-order kinetic model which corresponds to chemisorption as a rate limiting mechanism. The calculated q_e values correspond well to the real values at given Cd^{2+} concentrations with high regression coefficients. The adsorption equilibrium data are well represented by the Freundlich model. The new economical reinforced and porous hybrid gelled beads can therefore be used to eliminate heavy metals since the process of adsorption of Cd^{2+} by the F2 beads (SA-PVA-$CaCO_3$-Al-Mt) has shown a strong and rapid adsorption of cadmium.

References

[1] R. Verma, A. Asthana, A.K. Singh, S. Prasad, Md. A.B.H. Susan, Novel glycine-functionalized magnetic nanoparticles entrapped calcium alginate beads for effective removal of lead, Microchem. J., 130 (2017) 168–178.
[2] Z.-G. Cui, K. Ahmed, S.F. Zaidi, J.S. Muhammad, Ins and outs of cadmium-induced carcinogenesis: mechanism and prevention, Cancer Treat. Res. Commun., 27 (2021) 100372, doi: 10.1016/j.ctarc.2021.100372.
[3] H. Alyasi, H.R. Mackey, K. Loganathan, G. McKay, Adsorbent minimisation in a two-stage batch adsorber for cadmium removal, J. Ind. Eng. Chem., 81 (2020) 201–208.
[4] I. Suhani, S. Sahab, V. Srivastava, R.P. Singh, Impact of cadmium pollution on food safety and human health, Curr. Opin. Toxicol., 27 (2021) 1–7.
[5] Y. Ma, D. Ran, X. Shi, H. Zhao, Z. Liu, Cadmium toxicity: a role in bone cell function and teeth development, Sci. Total Environ., 769 (2021) 144646, doi: 10.1016/j.scitotenv.2020.144646.
[6] C.F. Mok, Y.C. Ching, F. Muhamad, N.A. Abu Osman, N.D. Hai, C.R.C. Hassan, Adsorption of dyes using poly(vinyl alcohol) (PVA) and PVA-based polymer composite adsorbents: a review, J. Polym. Environ., 28 (2020) 775–793.

[7] H.A. Aziz, N. Othman, M.S. Yusuff, D.R.H. Basri, F.A.H. Ashaari, M.N. Adlan, F. Othman, M. Johari, M. Perwira, Removal of copper from water using limestone filtration technique: determination of mechanism of removal, Environ. Int., 26 (2001) 395–399.
[8] K. Ahmad, I.A. Bhatti, M. Muneer, M. Iqbal, Z. Iqbal, Removal of heavy metals (Zn, Cr, Pb, Cd, Cu and Fe) in aqueous media by calcium carbonate as an adsorbent, Int. J. Chem. Biochem. Sci., 2 (2012) 48–53.
[9] M.S. Tizo, L.A.V. Blanco, A.C.Q. Cagas, B.R.B. Dela Cruz, J.C. Encoy, J.V. Gunting, R.O. Arazo, Efficiency of calcium carbonate from eggshells as an adsorbent for cadmium removal in aqueous solution, Sustainable Environ. Res., 28 (2018) 326–332.
[10] L. Yang, Y. Li, H. Hu, X. Jin, Z. Ye, Y. Ma, S. Zhang, Preparation of novel spherical PVA/ATP composites with macroreticular structure and their adsorption behavior for Methylene blue and lead in aqueous solution, Chem. Eng. J., 173 (2011) 446–455.
[11] Z. Mahmood, A. Amin, U. Zafar, M.A. Raza, I. Hafeez, A. Akram, Adsorption studies of cadmium ions on alginate–calcium carbonate composite beads, Appl. Water Sci., 7 (2017) 915–921.
[12] F.V. Hackbarth, F. Girardi, J.C. Santos, A.A.U. de Souza, R.A.R. Boaventura, S.M.A. Guelli U. de Souza, V.J.P. Vilar, Ion-exchange breakthrough curves for single and multi-metal systems using marine macroalgae *Pelvetia canaliculata* as a natural cation exchanger, Chem. Eng. J., 269 (2015) 359–370.
[13] H. Demey, T. Vincent, E. Guibal, A novel algal-based sorbent for heavy metal removal, Chem. Eng. J., 332 (2018) 582–595.
[14] M. Ahmad, S. Ahmed, B.L. Swami, S. Ikram, Adsorption of heavy metal ions: role of chitosan and cellulose for water treatment, Int. J. Pharmacognosy, 2 (2015) 280–289.
[15] D. Dou, D. Wei, X. Guan, Z. Liang, L. Lan, X. Lan, P. Liu, H. Mo, P. Lan, Adsorption of copper(II) and cadmium(II) ions by in situ doped nano-calcium carbonate high-intensity chitin hydrogels, J. Hazard. Mater., 423 (2022) 127137, doi: 10.1016/j.jhazmat.2021.127137.
[16] H. Khalaf, O. Bouras, V. Perrichon, Synthesis and characterization of Al-pillared and cationic surfactant modified Al-pillared Algerian bentonite, Microporous Mater., 8 (1997) 141–150.
[17] O. Bouras, J.-C. Bollinger, M. Baudu, H. Khalaf, Adsorption of diuron and its degradation products from aqueous solution by surfactant-modified pillared clays, Appl. Clay Sci., 37 (2007) 240–250.
[18] R. Kummert, W. Stumm, The surface complexation of organic acids on hydrous γ-Al_2O_3, J. Colloid Interface Sci., 75 (1980) 373–385.
[19] S.R. Sudhamani, M.S. Prasad, K. Udaya Sankar, DSC and FTIR studies on gellan and polyvinyl alcohol (PVA) blend films, Food Hydrocolloids, 17 (2003) 245–250.
[20] H.S. Mansur, C.M. Sadahira, A.N. Souza, A.A.P. Mansur, FTIR spectroscopy characterization of poly(vinyl alcohol) hydrogel with different hydrolysis degree and chemically crosslinked with glutaraldehyde, Mater. Sci. Eng., C, 28 (2008) 539–548.
[21] N.S. Labidi, A. Djebaili, Studies of the mechanism of polyvinyl alcohol adsorption on the calcite/water interface in the presence of sodium oleate, J. Miner. Mater. Charact. Eng., 7 (2008) 147–161.
[22] F. Tomul, S. Balci, Synthesis and characterization of al-pillared interlayered bentonites, G.U. J. Sci., 21 (2007) 21–31.
[23] Z. Qiusheng, L. Xiaoyan, Q. Jin, W. Jing, L. Xuegang, Porous zirconium alginate beads adsorbent for fluoride adsorption from aqueous solutions, RSC Adv., 5 (2015) 2100–2112.
[24] M. Fertah, A. Belfkira, E.M. Dahmane, M. Taourirte, F. Brouillette, Extraction and characterization of sodium alginate from Moroccan *Laminaria digitata* brown seaweed, Arabian J. Chem., 10 (2017) S3707–S3714.
[25] R. Kumar, J. Chawla, Removal of cadmium ion from water/wastewater by nano-metal oxides: a review, Water Qual. Exposure Health, 5 (2014) 215–226.
[26] T. Dong, H. Xing, H. Wu, Y. Lv, L. Wu, S. Mi, L. Yang, Preparation of magnetic Levextrel resin for cadmium(II) removal, Environ. Technol. Innovation, 23 (2021) 101657, doi: 10.1016/j.eti.2021.101657.
[27] C. Harripersadth, P. Musonge, Y.M. Isa, M.G. Morales, A. Sayago, The application of eggshells and sugarcane bagasse as potential biomaterials in the removal of heavy metals from aqueous solutions, S. Afr. J. Chem. Eng., 34 (2020) 142–150.
[28] R. Liu, B. Lian, Immobilisation of Cd(II) on biogenic and abiotic calcium carbonate, J. Hazard. Mater., 378 (2019) 120707, doi: 10.1016/j.jhazmat.2019.05.100.
[29] R. Sasamoto, Y. Kanda, S. Yamanaka, Difference in cadmium chemisorption on calcite and vaterite porous particles, Chemosphere, 297 (2022) 134057, doi: 10.1016/j.chemosphere.2022.134057.
[30] J. Crank, The Mathematics of Diffusion, Clarendon Press, Oxford, 1975.
[31] C.H. Giles, T.H. MacEwan, S.N. Nakhwa, D. Smith, 786. Studies in adsorption. Part XI. A system of classification of solution adsorption isotherms, and its use in diagnosis of adsorption mechanisms and in measurement of specific surface areas of solids, J. Chem. Soc., 786 (1960) 3973–3993.
[32] M. Basu, A.K. Guha, L. Ray, Adsorption behavior of cadmium on husk of lentil, Process Saf. Environ. Prot., 106 (2017) 11–22.
[33] G.D. Angelis, L. Medeghini, A.M. Conte, S. Mignardi, Recycling of eggshell waste into low-cost adsorbent for Ni removal from wastewater, J. Cleaner Prod., 164 (2017) 1497–1506.
[34] A. Saeed, M. Iqbal, M.W. Akhtar, Removal and recovery of lead(II) from single and multimetal (Cd, Cu, Ni, Zn) solutions by crop milling waste (black gram **husk),** J. Hazard. Mater., 117 (2005) 65–73.